Supplementary material

Semi-liquid-stated flux assisted synthesis of CdS for boosting photocatalytic hydrogen evolution

Xiaoyan Xiang, Huanmin Liu, Kangle Lv, Dingguo Tang, Qin Li*

Key Laboratory of Catalysis and Energy Materials Chemistry of Ministry of Education & Hubei Key Laboratory of Catalysis and Materials Science & Key Laboratory of Analytical Chemistry of the State Ethnic Affairs Commission, South-Central Minzu University, Wuhan 430074, China

*Corresponding author.

E-mail address: liqin0518@mail.scuec.edu.cn (Q. Li).

1. Characterizations

The crystal structure of the catalysts were identified by powder X-ray diffraction (XRD, D8 Advance, Bruker) with a monochrome Cu Kα generator (λ = 1.5406 Å). The morphologies of the samples were observed on field emission scanning electron microscopy (FESEM, SU8010, Hitachi). X-ray photoelectron spectroscopy (XPS) was tested on the Escalab 250xi spectrometer (Thermo Scientific). The electron paramagnetic resonance (EPR) spectra were acquired by a Germany Bruker MS-5000 spectrometer. UV–visible diffuse reflectance spectroscopy (UV–vis DRS) was measured on an UV–visible spectrophotometer (UV2550, Shimadzu). Photoluminescence (PL) spectra were obtained using a fluorescence spectrophotometer (F-7000, Hitachi), with an excitation wavelength of 245 nm. The surface photovoltage (SPV) spectrometer CHF-XM500 produced by ZOLIX Instrument Co., Ltd. was used for the SPV test. The high angle annular dark field

(HAADF) scanning/transmission electron microscope (STEM) image, and energy dispersive X-ray spectroscopy (EDS) mapping were implemented by a Thermo Scientific Talos F200S scanning/transmission electron microscope to observe the microstructure and the element distribution of the samples.

2. Photoelectrochemical measurements

Photoelectrochemical measurements including transient photocurrent response (TPR) and electrochemical impedance spectroscopy (EIS) were carried out in a standard three-electrode cell by a CHI 760 electrochemical workstation (Shanghai Chenhua, China), using sample/ITO electrode, platinum-wire, and $Hg/HgCl_2$ electrode as the working, counter, and reference electrodes, respectively, and 0.5 M Na_2SO_4 aqueous solution (pH ≈ 5.45) was used as the electrolyte. The photocurrent was tested at -0.5 V bias voltage. A 420 nm LED (Shenzhen LAMPLIC Science Co. Ltd., China) was used as the visible-light source. Mott-Schottky measurement was carried out under direct current potential polarization at different fixed frequency of 1000, 2000, and 3000 Hz. The working electrode was prepared by adding a drop of sample slurry to the glassy carbon electrode.

3. Photocatalytic performance testing

The photocatalytic performance of the samples was investigated via testing H_2 production efficiency in an all glass automatic on-line trace gas analysis system (Labsolar-6A, Beijing Perfect Light Technology Co., Ltd.). A xenon lamp (300 W) with a 420 nm cut-off filter was used as the light source. The illumination area was ca. 33 cm^2, and the bulb was nine centimeters away from the top of the reaction solution. Before the hydrogen reaction, the 20 mg of the photocatalyst samples were uniformly dispersed in 80 mL of lactic acid (LA) aqueous solution (10 v%). During the photocatalytic reaction, 0.6 mL of the produced gas (H_2) was automatically collected every hour and injected into a gas chromatography (GC-2018, Shimazu, with TCD with 5 Å molecular sieve column, with N_2 as the carrier gas). The apparent quantum efficiency (AQE) was measured under the same photocatalytic reaction condition except that four 420 nm-LEDs (3 W) (Shenzhen LAMPLIC Science Co. Ltd. China) were used as light sources to trigger the photocatalytic reaction, instead of the Xenon lamp. The LEDs were positioned on the top of the reactor, 9 cm away from the top of the liquid, and the focused intensity on the flask for each of them was ca. 6.0 mW cm^{-2} over an area of 1 cm^2. The apparent quantum efficiency (AQE) was measured under the same photocatalytic reaction condition. The AQE was calculated according to Equation :

$$\text{AQE (\%)} = \frac{\text{number of evolved hydrogen molecules} \times 2}{\text{number of incident photons}} \times 100\ \%$$

4. Computational method

DFT calculations were conducted through the Vienna ab initio Simulation Package (VASP) with the projector augment wave method. Generalized gradient approximation of the Perdew-Burke-Ernzerhof (PBE) functional was used as the exchange-correlation functional. The Brillouin zone was sampled with 2 × 2 × 2 K points. The cutoff energy was set as 500 eV, and structure relaxation was performed until the convergence criteria of energy and force reached 1×10^{-5} eV and 0.02 eV $Å^{-1}$, respectively. A vacuum layer of 15 Å was constructed to eliminate interactions between periodic structures of surface models.

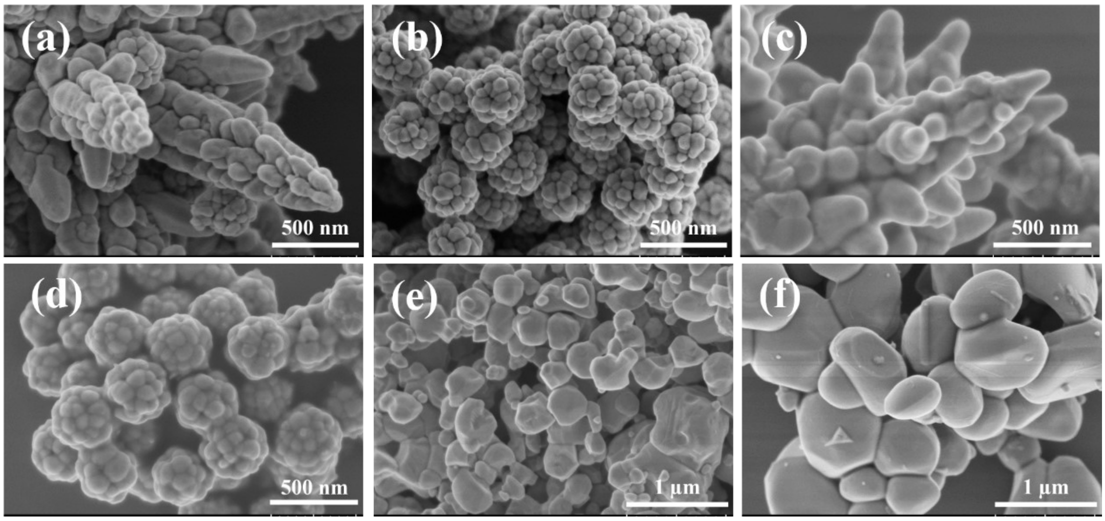

Fig. S1. FESEM images of the (a-b) CdS, (c-d) CdS-500, (e) CdS-Na500, and (f) CdS-K500 samples.

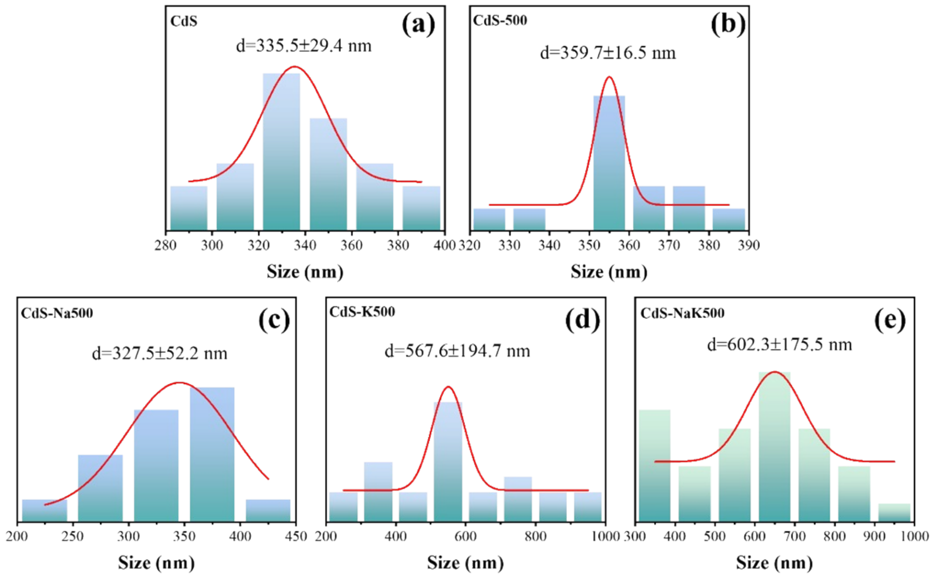

Fig. S2. Particle size distribution of (a) CdS, (b) CdS-500, (c)CdS-Na500, (d) CdS-K500 and (e) CdS-NaK500 samples. (These data were obtained from the previous SEM figures)

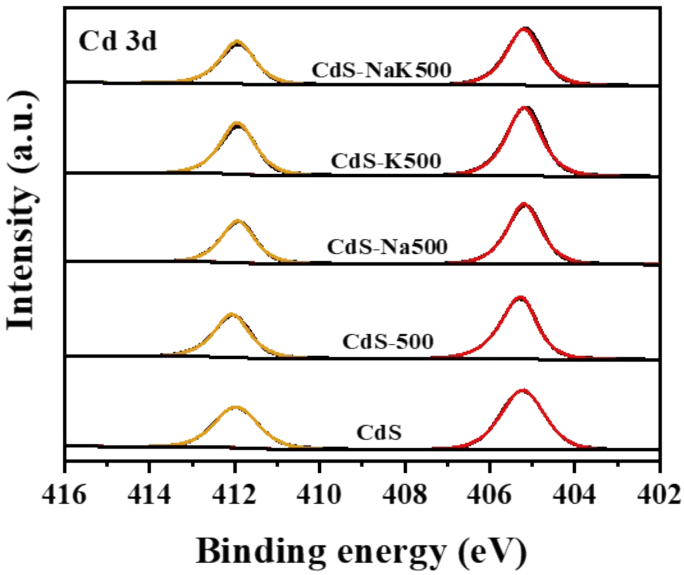

Fig. S3. Cd 3*d* XPS spectra of the prepared samples

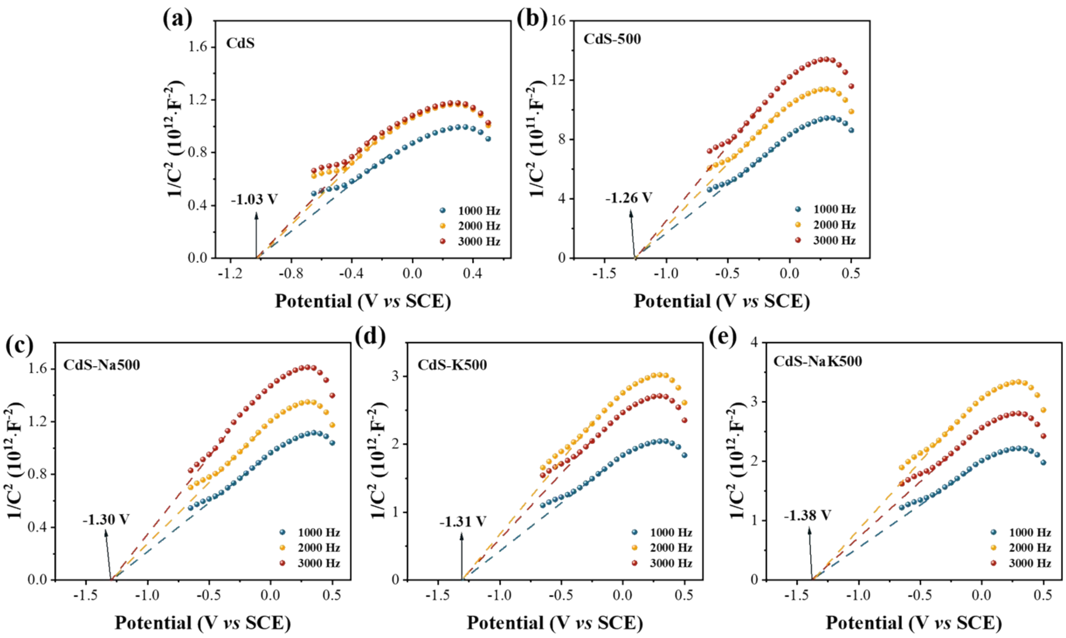

Fig. S4. Mott–Schottky plots of the (a) CdS, (b) CdS-500, (c) CdS-Na500, (d) CdS-K500 and (e) CdS-NaK500 samples.

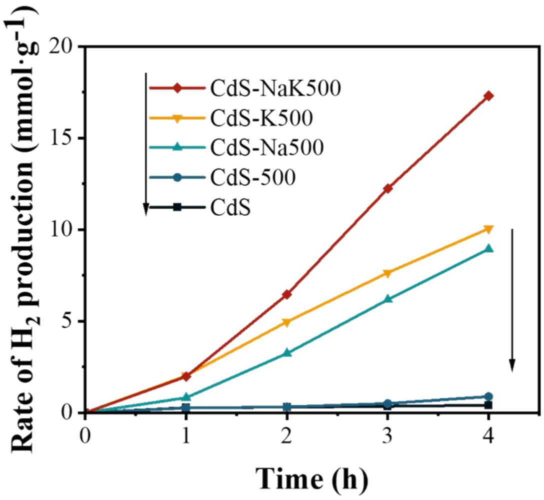

Fig. S5. Dependence of the amount of H_2 production on the time of the samples

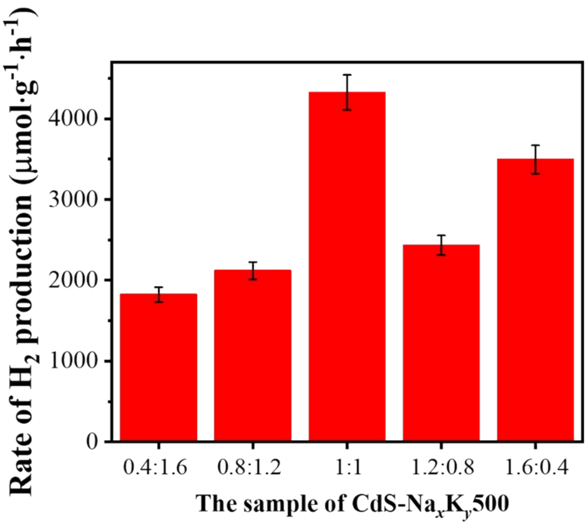

Fig. S6. Comparison of photocatalytic H_2-production rates of the CdS-Na_xK_y500 samples

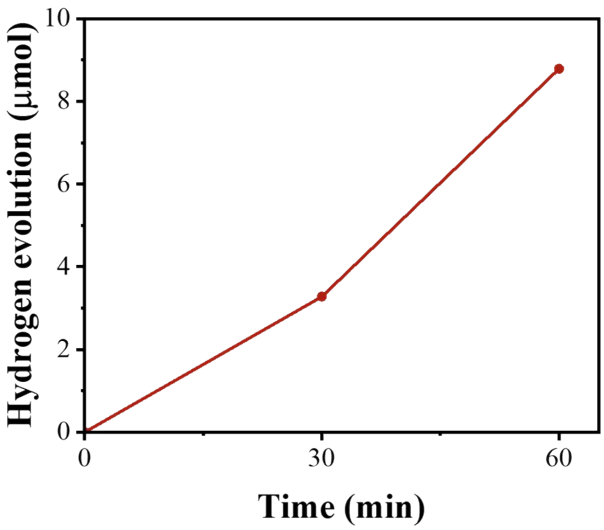

Fig. S7. Time course of the hydrogen evolution amount during the test of AQE at 420 nm.

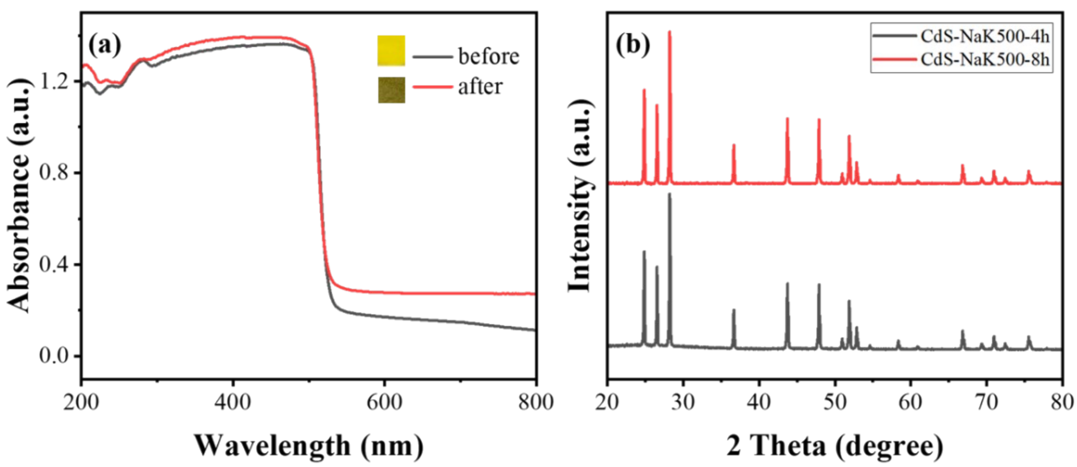

Fig. S8. (a) UV-vis light absorption spectra of the CdS-NaK500 sample before and after 4 h HER test. (b) XRD patterns of the CdS-NaK500 sample after 4 h and 8 h HER test.

Table S1. Comparison of the performance of CdS photocatalysts prepared via heat treatment for photocatalytic H_2 production

Photocatalyst	Heat treatment condition	Mass ratio of co-catalyst to CdS	Sacrificial reagent	Light source	R_{H_2} ($\mu mol\cdot h^{-1}\cdot g^{-1}$)	AQE at 420 nm	Enhancement factor to bare CdS for R_{H_2} ($\mu mol\cdot h^{-1}\cdot g^{-1}$)	Ref.
CdS-NaK500	NaCl-KCl molten salts, 500 °C, 30 min	None	10 vt% lactic acid	Xe lamp (λ≥420 nm)	4325.0	18.6%	41.7	This work
CdS	NaCl-$CaCl_2$ molten salts 600 °C, <1 min	0.5 % Pt	0.1 M Na_2S/Na_2SO_3	Xe lamp (λ≥465 nm)	286.0	19.2%	47.7	[1]
CdS	200 °C, 5 h	None	20 vt% lactic acid	Xe lamp (λ≥420 nm)	376.9	10.6%	21.1	[2]
CdS/carbon nanofiber	400 °C, 30 min	None	0.1 M Na_2S/Na_2SO_3	Xe lamp (λ≥420 nm)	175.4	NP [a]	4.0	[3]
CdS	200 °C, 2 h	None	20 vt% lactic acid	LED (430 nm)	7998.1	NP	1.3	[4]
CdS	550 °C, 2 h	None	None	Xe lamp(λ≥420 nm)	866.7	8.1%	NP	[5]

[a] NP means not provided.

Table S2. The formation energies data involved in the theoretical calculations for cubic CdS samples

E (cub-CdS)	$E_{gas}(Cl_2)$	E(Cl-cub-CdS)	E_{bulk} (S)	ΔE_{form}(Cl-cub-CdS)
-212.46 eV	-1.79 eV	-209.45 eV	-4.24 eV	0.56 eV

Table S3. The formation energies data involved in the theoretical calculations for hexagonal CdS samples

E (hex-CdS)	$E_{gas}(Cl_2)$	E(Cl-hex-CdS)	E_{bulk} (S)	ΔE_{form}(Cl-hex-CdS)
-238.71 eV	-1.79 eV	-236.07 eV	-4.24 eV	0.18 eV

References

1 H. Nagakawa; T. Tatsuma. Highly crystalline wurtzite CdS prepared by a flux method and application to photocatalysis. *ACS Appl. Energy Mater.*, 2022, **5**(12), 14652-14657.

2 R. K. Chava; N. Son; M. Kang. Controllable oxygen doping and sulfur vacancies in one dimensional CdS nanorods for boosted hydrogen evolution reaction. *J. Alloys Compd.*, 2021, **873**(2021), 159797.

3 Y. K. Kim; M. Kim; S. H. Hwang; S. K. Lim; H. Park; S. Kim. CdS-loaded flexible carbon nanofiber mats as a platform for solar hydrogen production. *Int. J. Hydrogen Energy*, 2015, **40**(1), 136-145.

4 H. Nagakawa. Introduction and quantification of sulfide Ion defects in highly crystalline CdS for photocatalysis applications. *Phys. Status Solidi A*, 2024, 2400213.

5 X. Wang; Y. Zhang; S. Jiang; J. Su; S. Song. Localized CdS homojunctions with optimal ratio of high and low index facets to dynamically boost H_2O splitting into H_2 energy. *J. Mater. Sci. Technol.*, 2024, **171**(2024), 94-100.